DOI: 10.1002/vms3.834

ORIGINAL ARTICLE

WILEY

CT anatomy of the head in the Ile de France sheep

Majid Masoudifard[1] | Omid Zehtabvar[2] | Seyyed Hossein Modarres[3] | Fateme Pariz[3] | Mohsen Tohidifar[1]

[1]Department of Surgery and Radiology, Faculty of Veterinary Medicine, University of Tehran, Tehran, Iran

[2]Department of Basic Sciences, Faculty of Veterinary Medicine, University of Tehran, Tehran, Iran

[3]DVM Student, Faculty of Veterinary Medicine, University of Tehran, Tehran, Iran

Correspondence
Majid Masoudifard, Department of Surgery and Radiology, Faculty of Veterinary Medicine, University of Tehran, Tehran, Iran.
Email: mmfard@ut.ac.ir

Abstract

Background: CT scan images provide accurate anatomical data from different areas of the body that can be used to diagnose diseases.

Objectives: The present work aimed to describe the normal anatomical structures of the Ile de France sheep head and its morphometric and volumetric properties using computed tomography (CT) and stereological methods.

Methods: Five adult Ile de France sheep heads, which were of mature age (above 10 months), were included in this study. The different cavities of the head, including the nasal cavity, paranasal sinuses, oral cavity, orbital cavity and vestibulocochlear system, were evaluated using CT scans, cross, sagittal and coronal sections.

Results: The mean length, height and width of the skull were 25.3 ± 1.02, 9.8 ± 0.93 and 12.3 ± 0.91 cm, respectively. The results showed that the nasal cavity is divided into three regions. Vestibular, respiratory and olfactory regions. The paranasal sinuses are composed of maxillary, frontal, palatine, sphenoid, lacrimal and ethmoidal that were identified and named in the CT scan images and their corresponding anatomical cross-sections. The total volume of the head, nasal cavity and oral cavity was estimated to be 2998 ± 202.00, 303 ± 31.33 and 229.3 ± 10.61 cm^3, respectively.

Conclusions: The frontal sinus in the Ile de France sheep was limited to the frontal bone without extending into the parietal, temporal, or occipital bones, similar to Saanen goat. This study provided a comprehensive atlas of Ile de France sheep anatomy to internal medicine veterinarians and surgeons.

KEYWORDS
anatomy, computed tomography, Ile de France sheep, morphometric study, volumetric study

1 | INTRODUCTION

The superficial landmarks of anatomical features within the skull region are attributed to the genetic and environmental factors which might be helpful in interpreting extensive variety in the phenotyping between and within breeds or species. Accurate knowledge of the anatomical structure of the skull can be an effective aid in ontogenic studies as well as the determination of sexual polymorphisms. Identifying how different parts of the complex architecture of the head and its structures are interconnected has always been troublesome (Morrow et al., 2000).

Imaging modalities are valuable tools to overcome this problem and improve the knowledge of head anatomy. Given the strengths and weaknesses of each of these methods, they will be used for specific

This is an open access article under the terms of the Creative Commons Attribution-NonCommercial License, which permits use, distribution and reproduction in any medium, provided the original work is properly cited and is not used for commercial purposes.
© 2022 The Authors. *Veterinary Medicine and Science* published by John Wiley & Sons Ltd.

purposes. Superimposition of bony structures and cavities has made the radiography a weak technique for detecting the structures distinctly in normal or pathological conditions (Solano & Brawer, 2004). Computed tomography (CT) could be a reliable and non-invasive procedure for evaluating different pathological lesions or diseases within the head region as compared to the traditional radiography (Frazho et al., 2008). Although, this modality has been used widely for describing the normal structure of the head and other body regions in other animals (Frazho et al., 2008; Losonsky et al. 1997; Morrow et al., 2000), the combination of imaging techniques and stereological procedures has received little attention in veterinary practice.

This modality has previously been used to describe the anatomy of the paranasal sinuses and cranial cavity in some mammal species including equines (Arencibia et al., 2000; Tucker et al., 2016; Smallwood et al., 2002), carnivores (De Rycke et al., 2003; Reetz et al., 2006; Saunders et al., 2002) and non-mammal species like reptiles (Banzato et al., 2012). Moreover, among the ruminant species, the head anatomy of Egyptian buffalo (Alsafy et al., 2013), camel (Alsafy et al., 2014), Sambar deer (Keneisenuo et al., 2021), Rayini goat (Shojaei et al., 2008), Egyptian sheep (Awaad et al., 2019), Egyptian native goat (Seddek et al., 2014) and Saanen goat (Tohidifar et al., 2020) have been explained.

The Ile de France has been bred in France since 1822. The first Ile de France sheep arrived in South Africa in 1903. It was a present from Madame Arnaud Ginchard to the 'boere' of South Africa. These sheep were from the stud of the famous French breeder, Delacour of Gouzangrez. During the 1930s and 1970s, sheep were imported for research purposes, but again, this had no effect on the local sheep population. The first commercial Ile de France sheep were imported in 1972 by private breeders. Further imports founded the breed in South Africa. The Ile de France Breeders' Society was established in 1980. The Ile de France is a large, smooth-bodied, polled mutton sheep. It produces strong white wool of acceptable quality, free from coloured fibres (Snyman, 2014). Ile de France sheep is one of the meat-producing breeds and is especially popular among farmers due to its high twinning. As far as we know, the cross-sectional and CT atlas of the head regions in the Ile de France sheep have not been previously reported. Therefore, the present study was conducted to provide a detailed description of the head anatomy in this breed using gross anatomical sections and their corresponding CT images. Furthermore, the morphometric details and volume of the head cavities and structures in non-pathological conditions were estimated using design-based and unbiased stereological methods.

2 | MATERIALS AND METHODS

2.1 | Collection of the specimens

Heads of five adult apparent healthy sheep of both sexes (12 months, 65 ± 0.55 kg) were collected from one of the farms around Tehran province, Iran. Two samples were dead animals due to gastrointestinal and internal bleeding due to uterine rupture diseases and three specimens were slaughtered. The heads were separated from the second cervical vertebra and after complete washing, they were transferred to the Veterinary Teaching Hospital, Faculty of Veterinary Medicine, University of Tehran, Tehran, to obtain CT scan images. After preparing the CT scan images, they were kept in the cold storage of the anatomy department.

2.2 | Computed tomographic imaging

After preparation, the fresh samples were immediately examined using a helical scanner (Siemens Somatom-2 detectors, Germany. Kvp: 130 V-mAs: 77 and slice thickness: 1 mm). All CT images in the bone and soft tissue reconstruction algorithm were retrieved and reviewed using an image analysis workstation (Syngo MMWP VE40A). Afterward, 3D reconstruction was done using the RadiAnt DICOM Viewer software. The CT images corresponding to the anatomical cross-sections were found, and all anatomical structures seen in the CT images were labelled carefully.

2.3 | Preparation of the cross-sections

After CT scan imaging, three of the heads frozen at −20°C were serially sectioned using an electric band saw. Ten transverse sections with about 2.5 cm thickness were collected from each sample on average. One frozen head was cut sagittally. The caudal aspect of the sections was cleaned gently using a light brush under tap water. After cutting, the samples of each skull were specially placed in a 10% formalin solution. Sectional photographs were taken after the suggested time for the samples to be fixed (time of fixation: 6–18 h for biopsy specimens and 24–72 h for standard samples (Loomis & Alu-Protocol, 2016). All procedures were conducted according to the guidelines for the animal welfare approved by the ethic committee of the University of Tehran. The caudal surface of the sections was photographed using a digital camera (Nikon, D3400, 23 MP, Japan). The images were processed and anatomical structures were identified and labelled using Adobe Photoshop CC (Adobe system, 2022, San Jose, CA, USA).

2.4 | Morphometric study

The morphometry of the skull of this sheep was studied using the RadiAnt application (to estimate the morphometric details of hyoid bone, scalpel option in 3D mode in RadiAnt application was used). The results of the measurement are shown in Tables 3–6 and Figures 7–9. The factors used in this study were taken from 'A Morphometric Study on the Skull of Donkey (*Equus asinus*)' (Lei Zhu, 2014). Totally 26 parameters in the upper and lower skull are described in Table 2.

2.5 | Volumetric study

Volume measurement in RadiAnt and Digimzer software is done manually. To achieve the most accurate results, the volume calculation was

TABLE 1 Paranasal sinuses and their positions in the skull of Ile de France sheep, prominent structures within it and mentioned figures in this article

Paranasal sinus	Position	Prominent structures	Mentioned figure(s)
Frontal sinus	It lies from the level of second pre-molar tooth to 1.5 cm posterior to the orbital cavity.	Supra-orbital canal	4/3, 4, 5, 6, 7, 6/11
Maxillary sinus	It starts from the upper part of the first pre-molar tooth and continues in parallel with the maxillary teeth to about 1.3 cm caudal to the last molar one.	Infra - orbital canal, Nasolacrimal duct	2/10, 12, 3/8, 11, 12, 13, 14, 4/13, 6/12
Palatine sinus	This sinus is located above the soft palate of the first to third molar tooth.		2/12, 3/14
Sphenoid sinus	It was located inside the wing of pre-sphenoid bone, just below the brain cavity.		
Lacrimal sinus	This sinus is located near the middle of the frontal sinus and continues from the exit of the optic nerve from the eye ball to the front of the eye socket and the level of the first molar tooth.		3/5
Ethmoidal sinus	It is located at the end of the nasal cavity at level of second molar tooth and is connected to the brain wall.		4/14, 6/15
Dorsal conchal sinus	It starts from mid part of inter-alveolar space and extends to the front of the ethmoidal sinus.		2/3, ¾
Middle conchal sinus	It starts from the lateral edges of the nasal cavity in the area of the first molar tooth and continues along the dorsal conchal sinus, below it to the ethmoidal sinus.		3/9, 6/17
Ventral conchal sinus	Not found in this breed.		

performed automatically using the software available on the CT scan system (Syngo MMWP VE40A software). For this purpose, the study area was introduced to the software in bone window and the software automatically showed the boundaries of the study area in three available views (cross, sagittal and coronal sections) and, if approved, the volume per cubic centimetre was displayed to the nearest three decimal places. To increase the accuracy of the measurement, the average volume in all three existing views was examined.

3 | RESULTS

CT scans provided very clear bone window images of the head cavities including the nasal concha, nasal meatuses, conchal sinuses, paranasal sinuses, brain, eye and its appendices. The obtained results are provided in three sections. The anatomical features found in the CT scan or cross-sectional images are described in the first section and the morphometric measurements in the second section, and the volumetric values estimated in the head are presented in the last one.

3.1 | Computed tomographic and cross-sectional anatomy

In this section, nine transverse sections and two sagittal sections will be examined by showing CT scan images with corresponding anatomical cross-sections (Figures 1–6).

The nasal cavity is the facial part of the respiratory tract and extends from the osseous nasal opening to the cribriform plate of the ethmoid bone. It is separated longitudinally into two symmetric halves by the median nasal septum, which continues caudally in the perpendicular plate of the ethmoid bone and rostrally in the cartilaginous, flexible part of the nasal septum. Each half of the nasal cavity contains the nasal conchae rostrally and the ethmoidal labyrinth caudally (Figures 4/14, 6/15).

The nasal cavity ends in the nasopharyngeal meatus, which leads to the nasal part of the pharynx. The dorsal nasal concha is formed by the single basal leaf of the first endoturbinate, the middle nasal concha (concha nasalis media) is formed by the two spiral caves of the second endoturbinate and the ventral nasal concha is formed by the maxillary turbinate (Figures 1, 2). The protruding nasal conchae divide the nasal cavity into the dorsal nasal meatus between the dorsal nasal concha and the nasal roof, the middle nasal meatus between the dorsal nasal concha and the middle and ventral nasal conchae, which are arranged behind each other and the ventral nasal meatus between the middle and ventral nasal conchae and the nasal floor (Figures 1/5, 6/19).

The vomeronasal organ was bilaterally situated on each side of the ventral part of the cartilaginous nasal septum in the most rostral region of the nasal cavity that extended to the level of the first lower premolar tooth (Figures 1/9, 2/17). The nasal septum was completely cartilaginous and was dorsally in contact with the nasal and frontal bones. The nasal septum was ventrally located in the groove of the vomer bone and did not extend to the floor of the caudal nasal region (Figures 1/6, 2/8, 3/10, 4/16).

TABLE 2 Morphometric study

Parameters	Description	Mentioned figure(s)
Skull length (SL)	Measured as distance between the rostral point of the incisive bone to the external occipital protuberance of the occipital bone.	7
Skull height (SH)	Measured as distance from the summit of the frontal bone to the tip of the para-condylar process.	7
Skull width (SW)	Measured as distance between two zygomatic arches.	7
Cranial length (CL)	Distance between the nuchal crest and the cranial rims of the eyes.	7
Cranial width (CW)	Distance between the most lateral points of the cranial cavity at the level of the external acoustic meatus.	7
Facial length (FL)	Distance between the naso-frontal suture and the most rostral point of the incisive bone.	7
Orbital width (OW)	Equal to the diameter of the circle in which the eye is located.	
Mandibular height (MH)	A perpendicular line which connected the tip of the coronoid process to the ventral margin of the mandible.	8
Mandibular length (ML)	Measured as distance from the caudal margin of the ramus to the incisive teeth.	8
Diastema or inter-alveolar margin (D)	Distance between the most lateral incisive tooth and first pre-molar tooth.	
MFID	Distance from the mental foramen to the most lateral incisive tooth.	8
MFPD	Distance from the mental foramen to the cranial margin of the first pre-molar tooth.	8
MFVD	Distance from the mental foramen to the ventral margin of the mandibular body.	8
MFC	Distance from the caudal margin of the mandibular ramus to the mental foramen.	8
Incisor 1 length (I1)	Length of first left incisor.	7
Pre-Molar 1 length (PM1)	Length of first pre-molar tooth in mandible.	7
Pre-Molar 2 length (PM2)	Length of second pre-molar tooth in mandible.	7
Pre-Molar 3 length (PM3)	Length of third pre-molar tooth in mandible.	7
Molar 1 length (M1)	Length of first molar tooth in mandible.	7
Molar 2 length (M2)	Length of second molar tooth in mandible.	7
Molar 3 length (M3)	Length of third molar tooth in mandible.	7
Stylohyoid length (S)	Distance between styloid angle and the epihyoid.	9
Epihyoid length (E)	Distance between epihyoid and the ceratohyoid.	9
Ceratohyoid length (C)	Distance between ceratohyoid and the basihyoid.	9
Lingual process of the basihyoid bone length (LB)	Distance between the beginning and the end of this bone.	9
Thyrohyoid length (T)	Distance between Lingual process of the basihyoid and end of thyrohyoid bone.	9

Parameters, descriptions and mentioned Figure(s) in the skull of Ile de France sheep.

TABLE 3 Morphometric result of the head (unit of measurement is cm) in the Ile de France sheep

No.	SL	SH	SW	CL	CW	FL	OW	OCD
F1	26.3	10.8	13	10.2	6.5	19.3	6.3	0.37
F2	24.2	8.4	12.8	9.8	6.3	18.7	5.2	0.35
F3	26.5	9.3	13.3	9	6.8	19	6.4	0.34
M1	25.3	9.8	11	10.6	7.1	18.5	6.2	0.36
M2	24.4	10.7	11.5	10.4	7.2	17.7	5.2	0.36
Mean and SD, F	25.6 ± 1.05	9.5 ± 1.02	13 ± 0.22	10 ± 0.52	6.5 ± 0.2	19 ± 0.31	6 ± 0.55	0.35 ± 0.02
Mean and SD, M	24.8 ± 0.55	10.3 ± 0.55	11.3 ± 0.31	10.5 ± 0.12	7.2 ± 0.23	18.1 ± 0.42	5.7 ± 0.56	0.36 ± 0.00
Mean and SD, F&M	25.3 ± 1.02	9.8 ± 0.93	12.3 ± 0.91	10 ± 0.66	6.8 ± 0.32	18.6 ± 0.54	5.8 ± 0.56	0.35 ± 0.01

Skull length (SL), skull height (SH), skull width (SW), cranial length (CL), cranial width (CW), facial length (FL), orbital width (OW), optic canal diameter (OCN). F, Female, M, Male.

TABLE 4 Morphometric result of the teeth (unit of measurement is cm) in the Ile de France sheep

No.	I_1	PM_1	PM_2	PM_3	M_1	M_2	M_3
F1	0.7	0.6	0.8	1.3	1.5	1.6	1.6
F2	0.6	1	0.7	1.3	1.5	2	1.8
F3	0.5	0.8	0.8	1.2	1.8	1.5	1.4
M1	0.5	0.9	1	1.2	1.6	2	–
M2	0.6	0.6	0.8	1.1	1.7	1.6	1.7
Mean and SD, F	0.6 ± 0.061	0.8 ± 0.12	0.8 ± 0.05	1.3 ± 0.05	1.6 ± 0.12	1.7 ± 0.21	1.6 ± 0.15
Mean and SD, M	0.55 ± 0.02	0.75 ± 0.23	0.9 ± 0.15	1.15 ± 0.09	1.65 ± 0.05	1.8 ± 0.22	1.7 ± 0.05
Mean and SD, F&M	0.58 ± 0.01	0.78 ± 0.22	0.82 ± 0.16	1.22 ± 0.07	1.62 ± 0.12	1.74 ± 0.26	1.63 ± 0.13

Incisor 1 length (I1), pre-molar 1 length (PM1), pre-molar 2 length (PM2), pre-molar 3 length (PM3), molar 1 length (M1), molar 2 length (M2), molar 3 length (M3). F, Female, M, Male.

TABLE 5 Morphometric result of the mandible (unit of measurement is cm) in the Ile de France sheep

No.	MH	ML	D	MFID	MFPD	MFVD	MFC
F1	13	22	4.1	2.3	2.7	0.9	16.9
F2	11.3	19.6	3.9	1.9	2.5	0.7	14.8
F3	12.5	20.2	4	1.8	2.6	0.8	15.2
M1	13.5	21.9	3.2	2.2	2.4	0.9	14.3
M2	11.8	19.9	3.6	2.1	2.5	0.9	13.6
Mean and SD, F	12.3 ± 0.72	20.6 ± 1.21	4 ± 0.05	2 ± 0.21	2.6 ± 0.05	0.8 ± 0.06	15.6 ± 0.92
Mean and SD, M	12.6 ± 0.92	20.9 ± 1.56	3.4 ± 0.21	2.1 ± 0.05	2.5 ± 0.06	0.9 ± 0.00	14 ± 0.33
Mean and SD, F&M	12.4 ± 0.81	20.7 ± 1.06	3.8 ± 0.32	2 ± 0.25	2.5 ± 0.13	0.8 ± 0.12	15 ± 1.13

Mandibular height (MH), mandibular length (ML), diastema (D), distance from the mental foramen to the most lateral incisive tooth (MFID), distance from the mental foramen to the cranial margin of the first pre-molar tooth (MFPD), distance from the mental foramen to the ventral margin of the mandibular body (MFVD), distance from the caudal margin of the mandibular ramus to the mental foramen (MFC). F, Female, M, Male.

TABLE 6 Morphometric result of the hyoid bone (unit of measurement is cm) in the Ile de France sheep

No.	S	E	C	LB	T
F1	6	1.3	1.4	0.8	1.4
F2	5.4	1	1.4	0.8	1
F3	4.9	1	1.1	0.9	1
M1	5	1.2	1.3	1	1.1
M2	5.8	1.1	1.3	0.8	1.2
Mean and SD, F	5.4 ± 0.51	1.1 ± 0.15	1.3 ± 0.02	0.8 ± 0.06	1.1 ± 0.21
Mean and SD, M	5.4 ± 0.42	1.2 ± 0.02	1.3 ± 0.00	0.9 ± 0.16	1.2 ± 0.05
Mean and SD, F&M	5.4 ± 0.42	1.1 ± 0.13	1.3 ± 0.14	0.8 ± 0.08	1.14 ± 0.21

Stylohyoid length (S), Epihyoid length (E), Ceratohyoid length (C), Lingual process of the basihyoid bone length (LB), Thyrohyoid length (T). F Female, M Male.

Some skull bones have hollow cavities called paranasal sinuses. These cavities are different in different species and sometimes they are directly and indirectly related to each other. As the relevant clinical applications in correlation to the gross anatomy of the paranasal sinuses remain inadequate, especially in sheep, so, it is necessary to understand the definite position, extension and communication of these sinuses for improvement of the diagnosis of the upper respiratory tract disorders. The paranasal sinuses constituted maxillary, frontal, lacrimal and ethmoidal that were recognized and named in the CT scan images and their corresponding anatomical cross-sections. A summary of what is read below is in Table 1

It entirely occupied the frontal bone, extending rostrally within the lacrimal bone and caudally into the ethmoidal region of the nasal cavity. This sinus formed the rostro-dorsal and medial boundaries of the

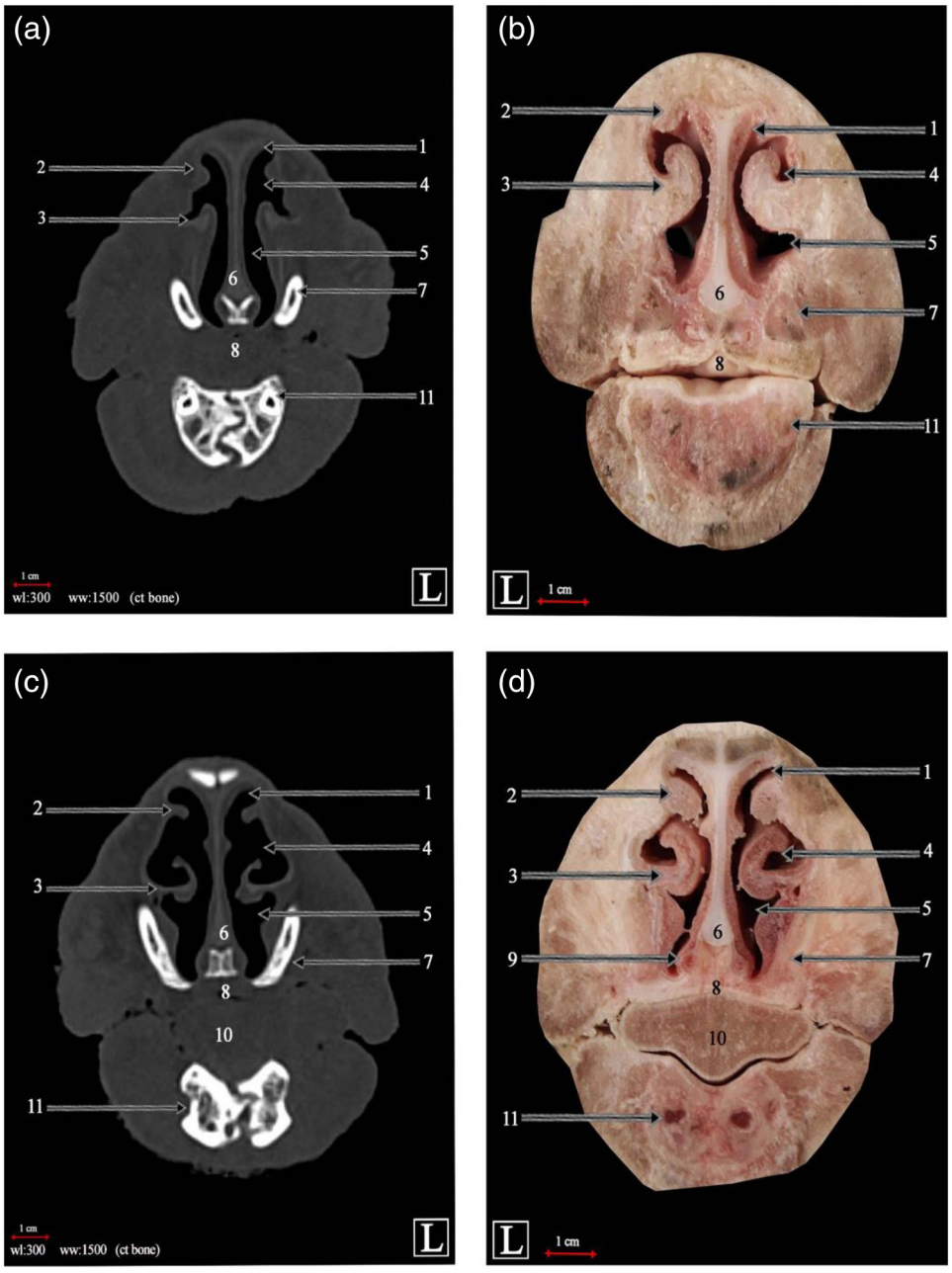

FIGURE 1 2D CT scan images (transverse view–bone window) and cross-sectional images in the Ile de France sheep. (a, b) At level of incisive teeth and (c, d) at level of inter-alveolar space. (1) Dorsal nasal meatus; (2) straight fold of dorsal nasal concha; (3) alar fold of ventral nasal meatus; (4) middle nasal meatus; (5) ventral nasal meatus; (6) nasal septum; (7) nasal process of incisive bone; (8) hard palate; (9) vomeronasal organ; (10) body of tongue; (11) mandible

orbital cavity and the rostro-dorsal boundary of the cranial cavity. The rostral frontal sinus was composed of three compartments including medial, intermediate and lateral ones (Figures 4/3,4,5,6, 6/1).

The maxillary sinus occupies a large part of the maxillary space and is located in the upper space of the maxillary teeth. The caudal part of dorsal compartment of maxillary sinus was in contact with the caudal part of the middle nasal meatus (Figure 3/11). The infra-orbital canal is also located in the middle of this sinus and connects the hole between supra- and infra-orbital foramen (Figures 2/12, 3/11,12,13,15, 4/13, 6/2).

The palatine sinus starts from the top of the first molar tooth and continues in parallel and in the ventromedial part of the maxillary sinus to the third molar tooth. It was exactly at the top hard plate and separated from nasal cavity with a thin wall (Figures 2/12, 3/14).

The sphenoidal sinus that extends to the wing of pre-sphenoid bone was very small in Ile de France sheep and was located just below the brain cavity.

The lacrimal sinus was a small excavation in the lacrimal bone and was separated from the lateral compartment of the rostral frontal sinus by a thin bony septum (Figure 3/5).

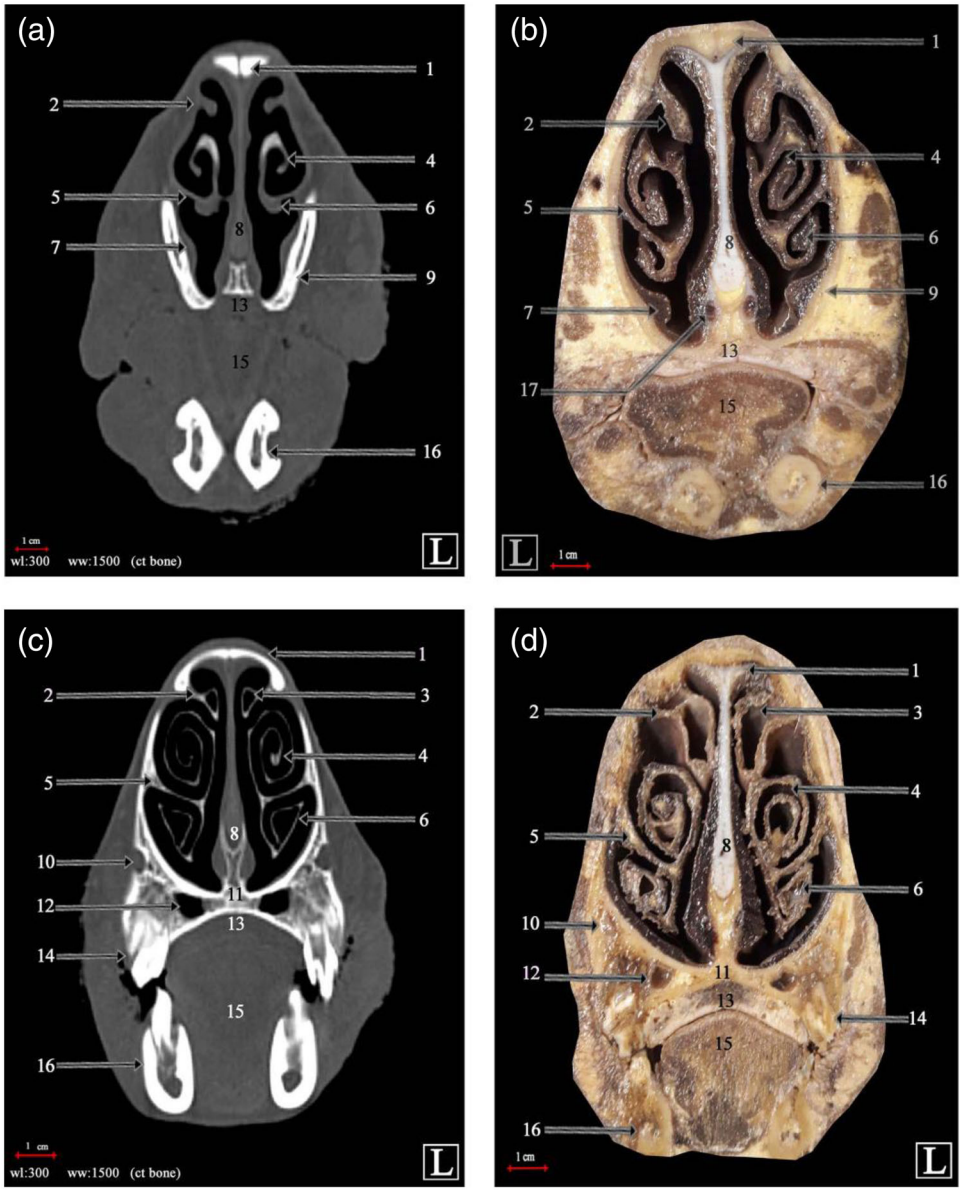

FIGURE 2 2D CT scan images (transverse view–bone window) and cross-sectional images in the Ile de France sheep. (a, b) At level of 1 cm rostral to the first pre-molar tooth and (c, d) at level of first pre-molar tooth. (1) Nasal bone; (2) dorsal nasal concha; (3) dorsal conchal sinus; (4) dorsal spiral lamella of ventral nasal concha; (5) ventral nasal concha; (6) ventral spiral lamella of ventral nasal concha; (7) basal fold of ventral nasal concha; (8) nasal septum; (9) nasal process of incisive bone; (10) infra-orbital canal; (11) palatine process of maxilla; (12) palatine sinus; (13) hard palate; (14) first pre-molar tooth; (15) body of tongue; (16) mandible; (17) vomeronasal organ

The conchal sinus is divided into three parts: dorsal, middle and ventral nasal sinus. Dorsal nasal sinus which is located on top of middle nasal, starts at the level of second pre-molar tooth to ethmoidal labyrinth (Figures 2/3, 3/4). The middle nasal sinus was present in this sheep breed, and it is below the final parts of dorsal nasal sinus (Figures 3/9, 6/17). The ventral conchal sinus was absent because of the presence of spiral lamellae within the caudal end of ventral nasal concha (Figures 2/4, 5, 6, 7, 3/6, 7, 21, 6/18).

There was a small excavation in the perpendicular plate of the ethmoidal bone which opened into the ethmoidal meatus. The right and left sinuses are completely separated. Each one was sub-divided by a small incomplete transverse septum into large rostral and small caudal partitions (Figures 4/14, 6/15).

Infra-orbital canal which incompletely divides maxillary sinus to the rostral and medial compartment, contains infra-orbital nerve, vein and artery. It begins from rostro-medial aspect of eye ball and within the direction of the rostro-medially continues parallel to the maxillary teeth.

Supra-orbital canal which accommodates the frontal nerve, vein and artery, begins from caudo-dorsal aspect of eye ball and continues rostro-medially. It ends at supra-orbital foramen with 4.7 mm diameter in frontal bone.

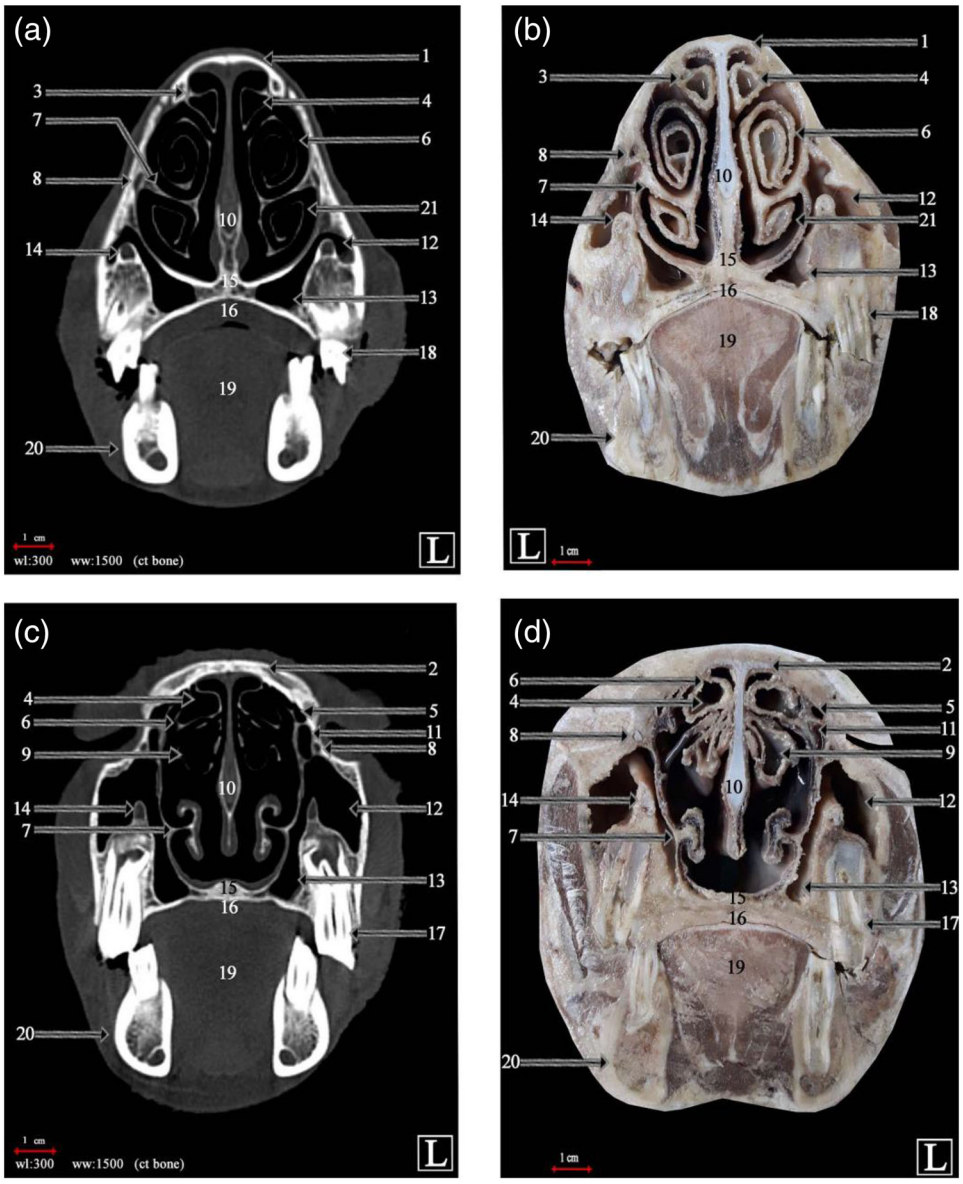

FIGURE 3 2D CT scan images (transverse view–bone window) and cross-sectional images in the Ile de France sheep. (a, b) At level of third pre-molar tooth and (c, d) at level of first molar tooth. (1) Nasal bone; (2) frontal bone; (3) dorsal nasal concha; (4) dorsal conchal sinus; (5) lacrimal sinus; (6) dorsal spiral lamella of ventral nasal concha; (7) ventral nasal concha; (8) nasolacrimal duct; (9) middle nasal sinus; (10) nasal septum; (11) dorsal compartment of maxillary sinus; (12) maxillary sinus; (13) palatine sinus; (14) infra-orbital canal; (15) palatine process of maxillary sinus; (16) hard palate; (17) second molar tooth; (18) third pre-molar tooth; (19) body of tongue; (20) mandible; (21) ventral spiral lamella of ventral nasal concha

The oral cavity is divided into anterior and posterior parts by the hard and soft palate. The hard palate forms the roof of the oral cavity in the anterior part and is limited to four pairs of incisors from the front and the inter-alveolar space is behind them (Figures 1/8, 2/13, 3/16, 6/21). After inter-alveolar, there are three pre-molar teeth on each side and then three molar teeth. The roof of the oral cavity forms the soft palate at the end, which eventually ends in the larynx (Figures 4/20, 5/7). The tongue occupies the greater part of the oral cavity but also extends into the oropharynx (Figures 1/10, 2/15, 3/19, 6/24).

The walls of the orbital cavity are composed of the frontal, lacrimal and zygomatic bones, the basisphenoid and the zygomatic process of the temporal bone. The rostro-medial wall of the orbital cavity is formed by the lacrimal bone. The orbit and its structures including eye ball layers (retina, choroid and sclera), lens, peri-orbital fat were recognized in the CT scan and anatomical sections as well (Figures 4/9,10,11).

The ear includes both auditory organs and balance. That is why it is the so-called vestibule-cochlear organ. The ear has three subdivisions: external ear, middle ear, internal ear. The organ of balance (vestibular system) is restricted to the internal ear. The external acoustic meatus has a distal cartilagenous part and a proximal osseous part. It begins with the narrowed part of the auricular cartilage.

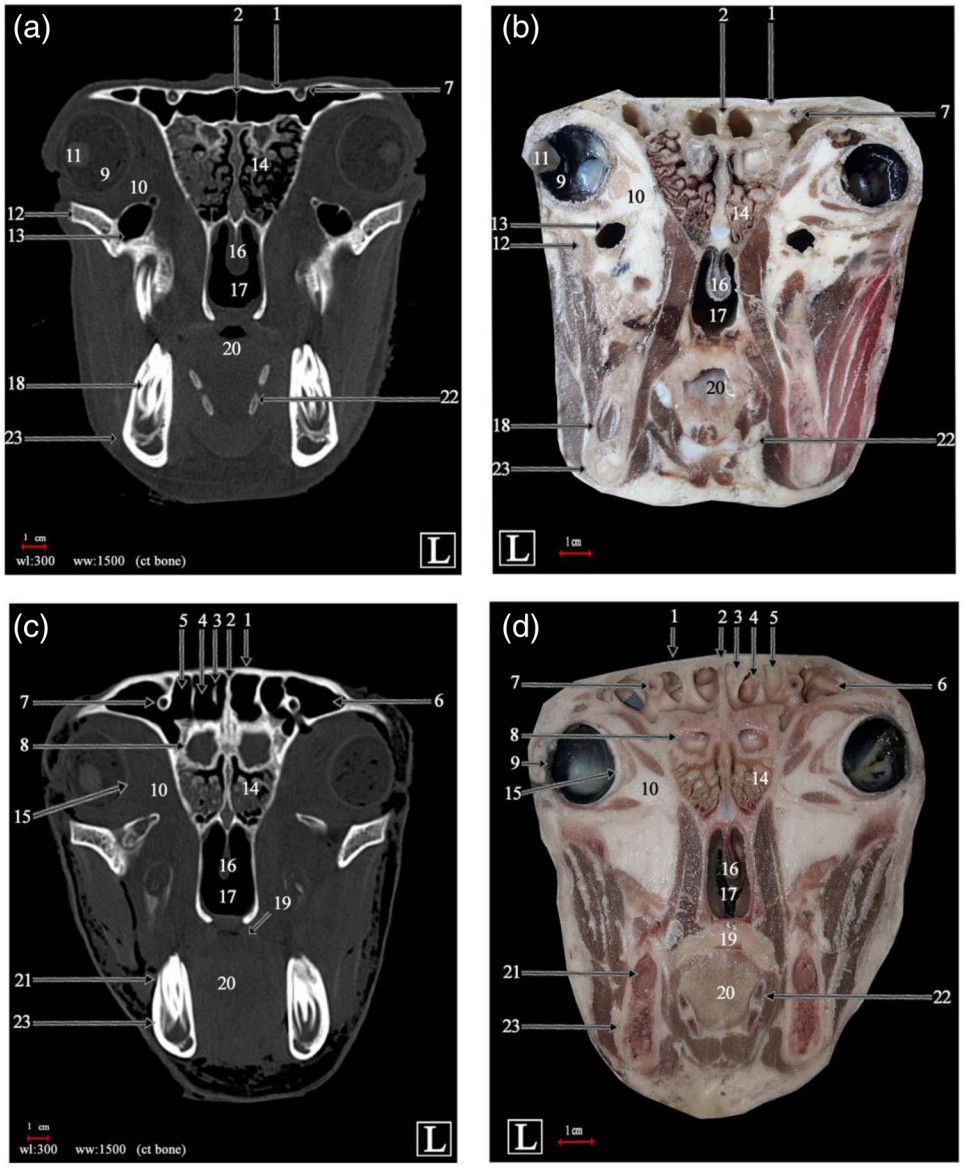

FIGURE 4 2D CT scan images (transverse view–bone window) and cross-sectional images in the Ile de France sheep. (a, b) At level of third molar tooth and (c, f) At level of eye ball centre. (1) Frontal bone; (2) inter-frontal septum; (3) medial compartment of rostral frontal sinus; (4) intermediate compartment of rostral frontal sinus; (5) lateral compartment of rostral frontal sinus; (6) rostral part of frontal sinus; (7) supra-orbital canal; (8) brain; (9) eye ball (retina and choroid); (10) periorbital fat; (11) lens of eye; (12) zygomatic arch; (13) maxillary sinus; (14) ethmoidal labyrinth; (15) sclera; (16) nasal septum; (17) choanae; (18) third molar tooth; (19) soft palate; (20) larynx; (21) root of last molar tooth; (22) hyoid bone; (23) mandible

It is lined with a stratified, squamous epithelium, which contains sebaceous and tubular ceruminous glands, which secrete earwax. In the ruminants, these glands are located within the cartilagenous part of the external acoustic meatus. The tympanic membrane, or eardrum, separates the middle ear from the external acoustic meatus. It transmits sound waves onto the auditory ossicles of the middle ear (Figure 6/3). The middle ear is comprised of: tympanic cavity, auditory ossicles and auditory tube. The tympanic cavity is housed within the petrous temporal bone. The ventral hypo-tympanicum, or tympanic bulla, is an enlarged bulbous expansion of the temporal bone. The transmission of vibrations from the tympanic membrane across the tympanic cavity to the inner ear is mediated by the three auditory ossicles.

A substantial median lingual process projects from the transverse basihyoid into the root of the tongue. From each end of the basihyoid, the thyrohyoid extends caudally to the thyroid cartilage of the larynx. The paired ceratohyoid articulates with the osseous epihyoid. The latter joins the hyoid apparatus to the head by forming a syndesmosis with the styloid process of the tympanic part of the temporal bone (Figures 4/22, 5/8, 9).

The lower jaw or mandible comprises two parts. Each half can be divided into body and ramus. The body of the mandible is divided into

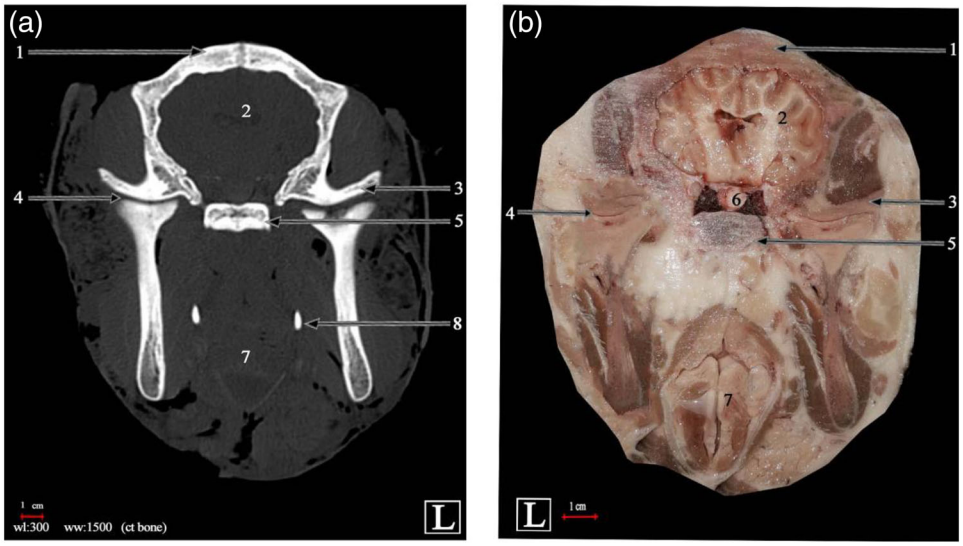

FIGURE 5 2D CT scan images (transverse view–bone window) and cross-sectional images in the Ile de France sheep. (a, b) At level of temporo-mandibular joint (TMJ). (1) Parietal bone, (2) brain, (3) zygomatic arch, (4) temporo-mandibular joint, (5) basilar part of occipital bone; (6) optic chiasma; (7) larynx; (8) hyoid bone

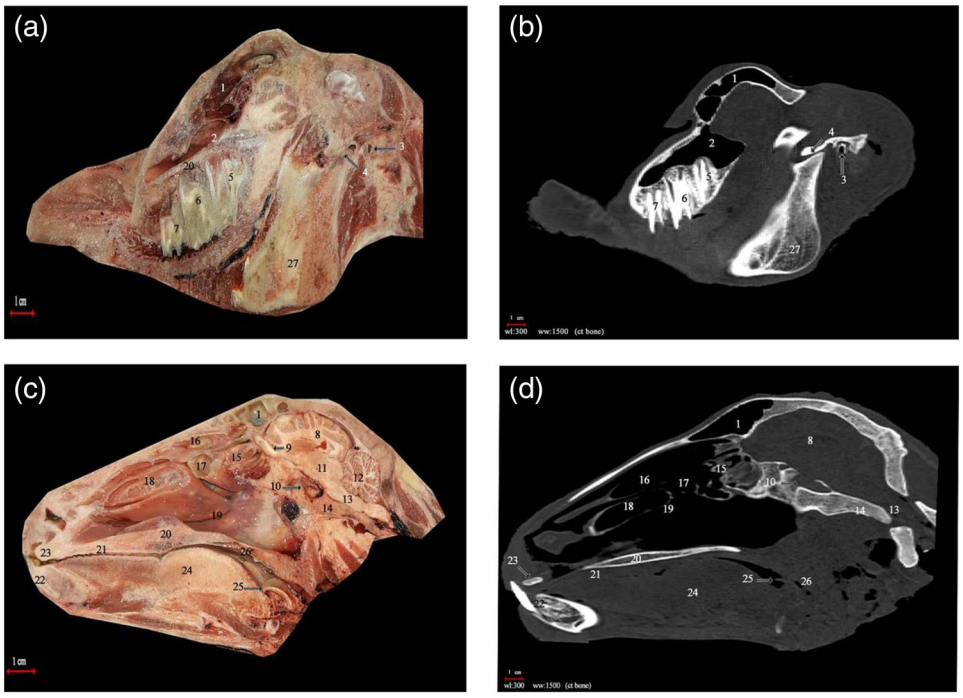

FIGURE 6 2D CT scan images (longitudinal view–bone window) and cross-sectional images in the Ile de France sheep. (a, b) At level temporo-mandibular joint (TMJ) and (c, d) At level of at level of medulla oblongata. (1) Frontal sinus; (2) maxillary sinus; (3) internal acoustic meatus; (4) temporo-mandibular joint; (5) third molar tooth of upper jaw; (6) second molar tooth of upper jaw; (7) first molar tooth of upper jaw; (8) brain; (9) olfactory bulb; (10) hypophyseal fossa; (11) inter-thalamic adhesion; (12) cerebellum; (13) medulla oblongata; (14) basisphenoid bone; (15) ethmoidal labyrinth; (16) dorsal nasal concha and its sinus; (17) middle nasal concha and its sinus; (18) ventral nasal concha and its sinus; (19) ventral nasal meatus; (20) palatine process of incisive bone; (21) hard palate; (22) incisor's tooth; (23) palatine process of incisive bone; (24) body of tongue; (25) epiglottis; (26) Soft palate; (27) Mandible

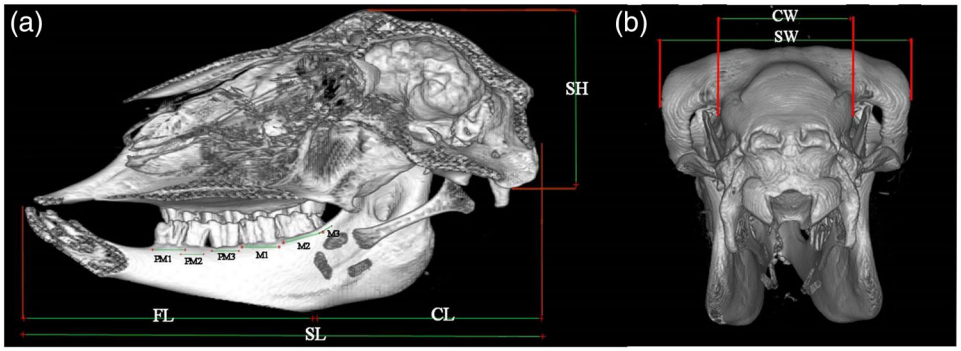

FIGURE 7 3D reconstruction (osseous-shaped-vp) in the Ile de France sheep. (a) Left median section, (b) caudal view. Morphometric parameters of the head. Skull length (SL), skull height (SH), skull width (SW), cranial length (CL), cranial width (CW), facial length (FL)

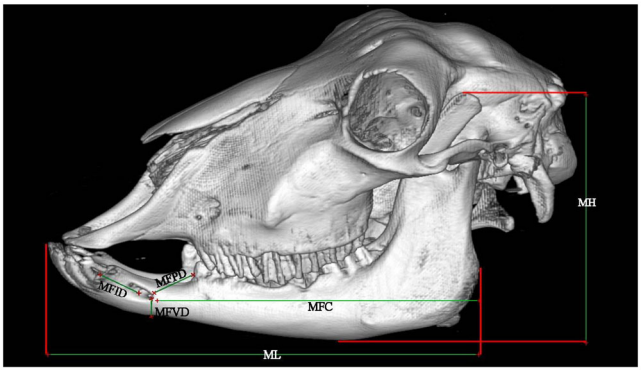

FIGURE 8 3D reconstruction (osseous-shaped-vp) lateral view in the Ile de France sheep. morphometric parameters of the Mandible. Mandibular height (MH), mandibular length (ML), distance from the mental foramen to the most lateral incisive tooth (MFID), distance from the mental foramen to the cranial margin of the first pre-molar tooth (MFPD), distance from the mental foramen to the ventral margin of the mandibular body (MFVD), distance from the caudal margin of the mandibular ramus to the mental foramen (MFC)

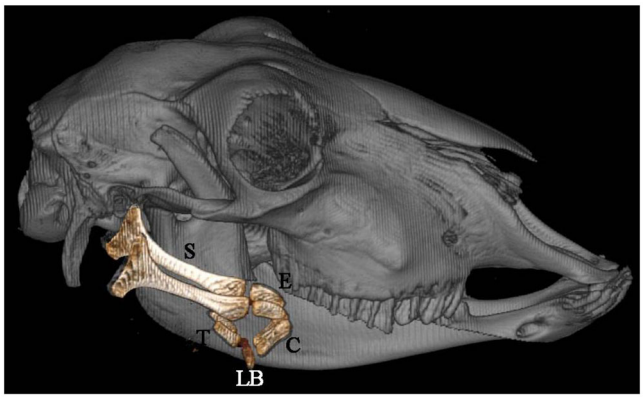

FIGURE 9 3D reconstruction (osseous-shaped-vp) lateral view in the Ile de France sheep. morphometric parameters of the hyoid bone. Stylohyoid length (S), epihyoid length (E), ceratohyoid length (C), lingual process of the basihyoid bone length (LB), thyrohyoid length (T)

anterior and posterior parts. The anterior part of mandible is convex and includes incisive teeth and the posterior part includes pre-molar and molar teeth. In this breed, as in other ruminants, there is a gap between the pre-molars and the incisors called inter-alveolar space or diastema (Figures 1/11, 2/16, 3/20). The ramus of mandible is wider and extends to the coronoid process which participates in temporo-mandibular joint (TMJ), dorsally and condylar and angular processes, caudally (Figures 4/23, 6/27, 8).

3.2 | Morphometric study

Morphometric information is data such as the length and width of anatomical structures as well as the distance of prominent organs in each. These data are very important to meet the demands of many surgeons and internal medicine veterinarians about the anatomy of the head in Ile de France sheep. The total skull length, height and width were 25.3 ± 1.02, 9.8 ± 0.93 and 12.3 ± 0.91 cm, respectively. Incisor's teeth in this breed were only in the mandible and there were four in each half of the jaw and the average of measured length was 0.58 ± 0.01 cm. The distance between auditory ossicles and external acoustic meatus was 2.16 ± 0.05 cm. Also, the distance between TMJ and auditory ossicles was 2.1 ± 0.12 cm. There were molars and pre-molars in the upper and lower jaws and three pre-molars and three molar teeth were observed in each half of the jaw. However, in one of the male samples, the last molar tooth was not observed. The mandible in the ruminants has the space between last incisor and first pre-molar tooth, called inter-alveolar space or diastema. The average length of the inter-alveolar space was 3.8 ± 0.32 cm. Reported numbers are mean ± SD.

3.3 | Volumetric study

The estimated values for total volume of the head and its cavities, cerebrum, cerebellum, paranasal and conchal sinuses in Ile de France sheep are presented in Tables 7 and 8. The mean total volume of the head was estimated to be 2998 ± 202.00 cm^3. While the volume of the nasal and oral cavities was estimated to be 303 ± 31.33 and 229.3 ± 10.61 cm^3, respectively, the mean value for the orbital cavity volume was

TABLE 7 Volumetric study of head (unit of measurement is cm^3) in the Ile de France sheep

No.	HV	NCV	OCV	OrCV	CerV	CereV	MIEV	HFV
F1	3189	325	238	58	97	39	14	4.2
F2	3049	338	233	56	94	33	11	3.8
F3	3212	303	239	59	96	38	11	4.5
M1	2860	315	221	58	90	35	15	4.2
M2	2680	248	215	51	84	33	13	4.3
Mean and SD, F	3150 ± 72.00	322 ± 14.55	236.6 ± 2.66	57 ± 1.22	95 ± 1.21	36.6 ± 2.63	12 ± 1.41	4.1 ± 2.82
Mean and SD, M	2770 ± 90.00	281.5 ± 33.52	218 ± 3.02	54.5 ± 3.56	87 ± 3.02	34 ± 1.02	14 ± 1.03	4.3 ± 0.03
Mean and SD, F&M	2998 ± 202.00	303 ± 31.33	229.3 ± 10.61	56.3 ± 3.22	92.1 ± 4.66	35.3 ± 2.65	12.8 ± 1.61	4.2±0.23

Head volume (HV), nasal cavity volume (NCV), oral cavity volume (OCV), orbital cavity volume in half skull (ORCV), cerebrum volume (CERV), cerebellum volume (CEREV), middle and internal ear volume in half skull (MIEV), hypophyseal fossa volume (HFV). F, Female, M, Male.

TABLE 8 Volumetric study of skull sinus (unit of measurement is cm^3) in the Ile de France sheep

No.	FSV	MSV	PS	LSV	DCSV	MCSV
F1	57	39	2	4	9	3.8
F2	59	34	3	5	10	4.5
F3	54	37	2.5	6	8	4.3
M1	56	32	2.3	5	7	5.6
M2	61	29	3.4	4	7	3.3
Mean and SD, F	56.6 ± 2.05	36.6 ± 2.03	2.5 ± 0.40	5 ± 0.83	9 ± 0.83	4.2 ± 0.31
Mean and SD, M	58.5 ± 2.52	30.5 ± 1.55	2.8 ± 0.55	4.5 ± 0.53	7 ± 0.00	4.5 ± 1.12
Mean and SD, F&M	57.5 ± 2.33	34 ± 4.66	2.6 ± 0.50	5 ± 1.55	8 ± 1.25	4.3 ± 0.75

Frontal sinus volume (FSV), maxillary sinus volume in half skull (MSV), palatine sinus in half skull (PS), lacrimal sinus volume in half skull (LSV), dorsal conchal sinus volume (DCSV), middle conchal sinus volume (MCSV), F, female, M, male.

estimated 56.3 ± 3.2 cm^3. The mean total volume of the cerebrum and cerebellum was 92.1 ± 4.66 and 35.3 ± 2.65 cm^3, respectively. The frontal sinus with the mean volume of 57.5 ± 2.33 cm^3 was the largest paranasal sinus and the lacrimal sinus with the mean volume of 5 ± 1.55 cm^3 was the smallest sinus in the Ile de France sheep. The ratios of frontal, maxillary and lacrimal sinuses to head volume were 0.019, 0.011 and 0.001, respectively. The ratio of dorsal nasal and middle nasal sinuses to nasal cavity volume was 0.026 and 0.014. Also, the hypophyseal fossa was measured in this breed was 4.2 ± 0.23 cm^3, which has not been reported in any other breeds. The results of the study from the volume of different areas in this sheep skull indicate that 10% of the volume of the head is the nasal cavity, 8% is the oral cavity and about 2% is each of the eye cavities. Also, about 4% of the total volume of the head is occupied by the cerebrum and cerebellum. The rate of standard deviation in the measurements was less than 5%. Reported numbers are mean ± DV.

4 | DISCUSSION

In this study, the anatomical structures of the head and their relationship with morphometric and volumetric measurements were investigated and presented as the Comprehensive Atlas of Ile de France sheep Anatomy to internal medicine veterinarians and surgeons.

The obtained CT scans with their spatial resolution gave better discrimination between the bone and soft tissue allowing differential appearance between the nasal and paranasal sinuses and other head cavities in sheep (Probst et al., 2005), in buffalo and in Saanen goat (Tohidifar et al., 2020). Because cortical bone and air have no signal on MRI (magnetic resonance imaging) sequences, an analysis of the normal anatomy of sinus cavity is difficult with MRI. CT, however, excels at assessing cortical bone. Subtle increases in mucosal thickness can be appreciated on CT because the surrounding air and bone are of such different radiodensities (Branstetter & Weissman, 2005).

The present study revealed two nasal conchal sinuses in the Ile de France sheep that occupied the dorsal and middle conchal sinus. This condition was in contrast to those reported in buffalo (Alsafy et al., 2013), camel (Alsafy et al., 2014), Egyptian sheep (Awaad et al., 2019) and Saanen goat (Tohidifar et al., 2020). The ventral conchal sinus was absent because of the presence of spiral lamellae within the caudal end of ventral nasal concha. The dorsal nasal concha in the Ile de France sheep opened directly into the ethmoidal meatus of the nasal cavity similarly in Saanen goat (Tohidifar et al., 2020). On the contrary, it has been reported that in buffalo (Alsafy et al., 2013) and sheep (Awaad

et al., 2019) this sinus communicated with the nasal cavity indirectly through the frontal sinus.

The present study showed that Ile de France sheep's head contained six paranasal sinuses, namely maxillary, frontal, palatine, sphenoid, lacrimal and ethmoidal sinuses. Because the relevant clinical applications in correlation to the gross anatomy of the paranasal sinuses remain inadequate, especially in sheep, so, it is necessary to understand the definite position, extension and communication of these sinuses for improvement the diagnosis of the upper respiratory tract disorders (Losonosky, Abbott, & Kuriashkin, 1997; Reetz et al., 2006). The palatine and sphenoidal sinuses were seen within the Ile de France sheep's head. Concerning the palatine and sphenoidal sinuses, there is a variable status in different ruminant breeds. The palatine sinus which was previously identified in buffalo (Alsafy et al., 2013), Iraqi local goat (Kareem & Sawad, 2016), Rayini goat (Shojaei et al., 2008) and sheep (May, 1970; Sisson & Grossman, 1975) are similar to our findings and those that are recorded in camel (Alsafy et al., 2014) and Egyptian sheep (Awaad et al., 2019). Regarding the sphenoidal sinus, it was absolutely recognized in camel (Alsafy et al., 2014), Egyptian sheep (Awaad et al., 2019) and buffalo (Alsafy et al., 2013). However, palatine and sphenoid sinuses were not observed in goat (May, 1970; Sisson & Grossman, 1975; Tohidifar et al., 2020), buffalo (Alsafy et al., 2013), camel (Alsafy et al., 2014) and cattle (Basso et al., 2016).

The frontal sinus in the Ile de France sheep was limited to the frontal bone, without extending into the parietal, temporal or occipital bones similar to Saanen goat (Tohidifar et al., 2020). This observation was in contrast to the findings of Awaad et al. (2019) in Egyptian sheep and in buffalo (Alsafy et al., 2013; Saigal et al., 1977), in which frontal sinuses were enclosed by the frontal and parietal bones. Moreover, the frontal sinus in giraffe (Badlangana et al., 2011) and ox was reported to begin in the frontal bone and extend caudally to the parietal and inter-parietal and to the temporal bones laterally. Therefore, the frontal sinus in large ruminants extends into the nuchal and lateral walls of the cranium with advancing age.

In this regard, the camel is an exception among the large ruminant species as its frontal sinus is restricted to the frontal bone (Alsafy et al., 2014). It is worth noting that the anatomy of the frontal sinus can be notably varied from horned ruminants to hornless ones. In the hornless breeds, such as Ile de France sheep, the frontal sinus is simply organized into two compartments with few septa and diverticula, while in the horned breeds, such as most goats, this sinus encompasses a complex architecture with numerous septa and inter-connected diverticula which caudally extended with various depths into the horn core. In horned animals, this issue should be considered for de-horning (El-hawari et al., 2015).

Contrary to Sisson and Grossman (1975) in small ruminants and Shojaei et al. (2008) in goats, which mentioned the extension of the maxillary sinus from the level of the first cheek tooth to the fourth cheek tooth, respectively, in this study the maxillary sinus extended from the level of the first pre-molar tooth to about 1.3 cm caudal to the last molar one just like Egyptian sheep (Awaad et al., 2019). In the CT scan and cross-sections of the skull of this breed, the maxillary sinus, contrary to the results of Awaad et al. (2019) and Tohidifar et al. (2020), Seddek et al. (2014), was not divided into lateral and medal compartment and only had the dorsal compartment of maxillary sinus in the caudo-lateral part of sinus. On the other hand, Awaad et al. (2019) and Tohidifar et al. (2020), Seddek et al. (2014) revealed that the maxillary sinus was incompletely divided by the **infra-orbital** canal into medial and lateral chambers.

The gross anatomy and CT in the current study, together with Sisson and Grossman (1975) in small ruminants and Shojaei et al. (2008), point to the presence of the palatine sinus in the small ruminant, which, unlike the palatine sinus in horses, is not associated with the sphenoid sinus. This was inconsistent with Awaad et al. (2019) and Tohidifar et al.'s (2020), Seddek et al. (2014) results (Probst et al., 2005).

In this study, as in Tohidifar et al. (2020) and Kareem and Sawad's (2016) studies, no association was found between the lecrimal sinus and the frontal and maxillary sinuses. However, in goat (Kareem & Sawad 2016) they considered this sinus as a part of the frontal sinus. In addition to that, Awaad et al. (2019) recorded a connection between the lacrimal and maxillary sinus by maxillo-lacrimal opening, while May (1970) noticed this sinus opened into the middle nasal meatus.

The naso-lacrimal duct is a soft tissue tube that passes through the lacrimal bone and the maxilla. Caudally, it begins from lacrimal foramen which is situated ventral to the facial crest (Masoudifard et al., 2008). Rostrally, it emerges from its honey canal and continues deep to the nasal mucosa on the nasal aspect of the maxilla. It ends by opening into the ventral nasal meatus at the level of first molar tooth.

Comparing the measured morphometric parameters between the male and female Ile de France sheep showed no significant differences.

The mean total skull length of the Ile de France sheep was found to be 25.3 ± 1.02 cm. Other studies reported 22.67± 0.93 cm for Saanen goat (Wang et al., 2021), 6.99 ± 1.59 cm for West African Dwarf goat (Olopade et al., 2005) and 18.67 ± 0.66 cm for Markhoz goat (Goodarzi & Hoseini, 2014). This shows that the entire skull length of the Ile de France sheep is longer than that of those goat species.

The infra-orbital canal ends at level of third pre-molar tooth in the Ile de France sheep and the results were similar to Tohidifar et al. (2020) and Awaad et al. (2019). The mean length of this canal was 6.5 ± 0.20 cm and its width was 4.3 mm, approximately. The **infra-orbital** foramen is the most palpable prominence which can be used as a superficial landmark to explore the **infra-orbital** nerve, and was located dorsal to the second pre-molar tooth, and it was in contrast with Saanen goat that is located dorsal to the first pre-molar tooth (Wang et al., 2021).

We found two different foramens related to supra-orbital foramen in this breed, one of which was larger and the other was short. The shorter began from the end of the large one and it ended in rostro-medial to the major supra-orbital foramen. It was approximately 1.6 mm in diameter. The length of this canal was 2.3 cm. No article was found about the mentioned multiple exits in supra-orbital foramen.

The volume of the head and its sub-components, including orbital, oral and nasal cavities as well as the volume of the cerebrum and cerebellum, were estimated in automatic method, measured by software available on the CT scan system (Syngo MMWP VE40A software). The Cavalieri method could be a powerful and efficient tool for estimating

the fractional and absolute volumes of different structures with regular or irregular geometrical shapes (Roberts et al., 2000). This method is easily applied to the MRI and CT images for volume estimation (Sahin & Ergur, 2006). It has been used less frequently for volume estimation of organs in normal or pathological conditions in veterinary medicine. Sadeghinezhad et al. (2018) have conducted a developmental study on the spinal cord of sheep embryo using stereological methods. More recently, the volumetric properties of the lumbo-sacral spinal cord in quail and thoracic spinal cord in ducks were investigated (Cakmak & Ragbetli, 2019; Cakmak & Karadag, 2019). Because the Cavalieri method was older and the CT scan software was more reliable, we decided to use the automatic method for volume calculations so as not to commit potential human errors in measurement and to increase accuracy. A measure of volume was also recorded at three causal levels to further increase accuracy.

The total volume of the head was 2998 ± 202.00 cm^3 and the volume of cerebrum and cerebellum was 92.1 ± 4.66, 35.3 ± 2.65 cm^3, approximately. The total volume of head, cerebrum and cerebellum was 1958 ± 205.4, 309.4 ± 57.2 and 77 ± 7.6 cm^3 in Saanen goat (Tohidifar et al., 2020).

Due to the limited resources on volume measurements in small ruminants, only one goat breed had a volume study of the head sinuses. To correctly compare the sinuses in these two species, the ratio of sinuses volume to each other can help us. The ratio of frontal sinus to maxillary in Ile de France sheep was 1.67, while this ratio was 1.65 in Saanen goats, indicating that the size ratio of these two sinuses is the same in these two species. Also, the ratio of cerebrum to cerebellum was 2.56 in Ile de France sheep and 4 in Saanen goat (Tohidifar et al., 2020). This indicates an increase in cerebrum volume relative to the cerebellum or a decrease in cerebellar volume relative to the cerebrum.

In conclusion, to the best of our knowledge, there is little information about these morphometric and volumetric parameters in the Ile de France sheep skull. Therefore, these findings provide basic data that would be useful for blocking terminal branches of the cranial nerves in this breed for surgical purpose or teeth injuries treatment. Also, the CT and cross-sectional anatomy are important to investigate the characteristic features of the paranasal sinuses as well as their relations and communications with the other cavities in the head region of the Ile de France sheep. Further studies using a wider range of animals and breeds are necessary to rule out intra- and inter-breed variations.

ACKNOWLEDGMENTS

The authors wish to express their appreciation to everyone who assisted in this study, especially the staff of the anatomy and radiology departments of the Faculty of Veterinary Medicine, University of Tehran.

CONFLICT OF INTEREST

The authors declare that they have no conflict of interest.

AUTHOR CONTRIBUTIONS

Majid masoudifard: conceptualization; resources. Omid Zehtabvar: conceptualization; resources. Seyyed Hossein Modarres: data curation, formal analysis. Fateme Pariz: data curation, methodology, writing–original draft. Mohsen Tohidifar: formal analysis; writing–original draft.

DATA AVAILABILITY STATEMENT

The data that support the findings of this study are available from the corresponding author upon reasonable request.

ETHICS STATEMENT

This study was a DVM thesis and all experimental procedures were approved by the Faculty of Veterinary medicine, University of Tehran Local Ethics Committee.

PEER REVIEW

The peer review history for this article is available at https://publons.com/publon/10.1002/vms3.834

ORCID

Majid Masoudifard https://orcid.org/0000-0001-9087-6919
Omid Zehtabvar https://orcid.org/0000-0002-4343-4453
Seyyed Hossein Modarres https://orcid.org/0000-0001-8940-3620
Fateme Pariz https://orcid.org/0000-0003-1274-793X
Mohsen Tohidifar https://orcid.org/0000-0002-4360-9874

REFERENCES

Alsafy, M. A., El-Gendy, S. A., & Abumandour, M. M. (2014). Computed tomography and gross anatomical studies on the head of one-humped camel (*Camelus dromedarius*). *Anatomical Record (Hoboken, N.J.: 2007)*, *297*(4), 630–642.

Alsafy, M. A., El-Gendy, S. A., & El Sharaby, A. A. (2013). Anatomic reference for computed tomography of paranasal sinuses and their communication in the Egyptian buffalo (*Bubalus bubalis*). *Anatomia, Histologia, Embryologia*, *42*(3), 220–231.

Arencibia, A., Vázquez, J. M., Rivero, M., Latorre, R., Sandoval, J. A., Vilar, J. M., & Ramírez, J. A. (2000). Computed tomography of normal cranioencephalic structures in two horses. *Anatomia, Histologia, Embryologia*, *29*(5), 295–299.

Awaad, A. S., Abdel Maksoud, M., & Fathy, M. Z. (2019). Surgical anatomy of the nasal and paranasal sinuses in Egyptian native sheep (*Ovis aries*) using computed tomography and cross sectioning. *Anatomia, Histologia, Embryologia*, *48*(4), 279–289.

Badlangana, N. L., Adams, J. W., & Manger, P. R. (2011). A comparative assessment of the size of the frontal air sinus in the giraffe (*Giraffa camelopardalis*). *Anatomical Record (Hoboken, N.J.: 2007)*, *294*(6), 931–940.

Banzato, T., Selleri, P., Veladiano, I. A., Banzato, T., Selleri, P., Veladiano, I. A., Martin, A., Zanetti, E., & Zotti, A. (2012). Comparative evaluation of the cadaveric, radiographic and computed tomographic anatomy of the heads of green iguana (*Iguana iguana*), common tegu (*Tupinambis merianae*) and bearded dragon (*Pogona vitticeps*). *BioMedCentral (BMC) Veterinary Research*, *8*, 53.

Basso, F. Z., Busato, E. M., Silva, J. R., Guedes, R. L., Filho, I. R., & Dornbusch, P. (2016). Comparison between three techniques for videosinuscopy in cattle. *Ciencia Rural*, *46*, 1262–1267.

Branstetter, B. F. 4th, & Weissman, J. L. (2005). Role of MR and CT in the paranasal sinuses. *Otolaryngologic Clinics of North America*, *38*(6), 1279–1299.

Çakmak, G., & Cetin Ragbetli, M. (2019). A stereological analysis on the calculation of the volume values of thoracic segments in ducks. *Anatomia*, *49*, 17–24.

Cakmak, G., & Karadag, H. (2019). A stereological study on calculation of volume values regarding lumbosacral segments of quails. *Anatomia, Histologia, Embryologia*, *48*(2), 164–174.

De Rycke, L. M., Saunders, J. H., Gielen, I. M., van Bree, H. J., & Simoens, P. J. (2003). Magnetic resonance imaging, computed tomography, and cross-sectional views of the anatomy of normal nasal cavities and paranasal sinuses in mesaticephalic dogs. *American Journal of Veterinary Research*, *64*(9), 1093–1098.

El-hawari, S. F., Elrashidy, M. H., & Mahmoud, M. E. (2015). Complications of horn overgrowth in sheep and goats with especial reference to their clinical behavior and surgical management. *Assuit Veterinary Medical Journal*, *61*, 131–138.

Frazho, J. K., Tano, C. A., & Ferrell, E. A. (2008). Diagnosis and treatment of dynamic closed-mouth jaw locking in a dog. *Journal of the American Veterinary Medical Association*, *233*(5), 748–751.

Goodarzi, N., & Shah Hoseini, T. (2014). Morphologic and osteometric analysis of the skull of markhoz goat (*Iranian angora*). *Veterinary Medicine International*, *2014*, 972682.

Kareem, D. A., & Sawad, A. A. (2016). Silicon polymer for cast of paranasal sinuses of Iraqi local goat (*Capra hircus*). *Basrah Journal of Veterinary Research*, *15*, 111–118.

Keneisenuo, K., Choudhary, O. P., Kalita, P. C., Duro, S., Kalita, A., Doley, P. J., Arya, R. S., Debroy, S., & Priyanka, P. (2021). A comparative study on the morphology, radiography and computed tomography of the skull bones of barking deer (*Muntiacus muntjak*) and sambar deer (*Rusa unicolor*). *Folia Morphologica*, *81*, 164–174.

Loomis, M., & Alu-Protocol, M. (2016). *Detailed discussion of tissue prep and formalin/formaldehyde fixation recommendations*. Experimental Pathology Research Laboratory Division of Advanced Research Technologies.

Losonsky, J. M., Abbott, L. C., & Kuriashkin, I. V. (1997). Computed tomography of the normal feline nasal cavity and paranasal sinuses. *Veterinary Radiology & Ultrasound: The Official Journal of the American College of Veterinary Radiology and the International Veterinary Radiology Association*, *38*(4), 251–258.

Masoudifard, M., Shojaei, B., & Vajhi, A. (2008). Radiographic anatomy of the head of sheep. *Iranian Journal of Veterinary Surgery*, *3*, 41–48.

May, N. D. (1970). *Anatomy of the sheep a dissection manual* (3rd ed.). University of Queensland Press.

Morrow, K. L., Park, R. D., Spurgeon, T. L., Stashak, T. S., & Arceneaux, B. (2000). Computed tomographic imaging of the equine head. *Veterinary Radiology & Ultrasound: The Official Journal of the American College of Veterinary Radiology and the International Veterinary Radiology Association*, *41*(6), 491–497.

Olopade, J., Olukayode, O., & Silas, K. (2005). Some aspects of the clinical anatomy of the mandibular and maxillofacial regions of the West African Dwarf goat in Nigeria. *International Journal of Morphology*, *23*(1), 33–36.

Probst, A., Henninger, W., & Willmann, M. (2005). Communications of normal nasal and paranasal cavities in computed tomography of horses. *Veterinary Radiology & Ultrasound: The Official Journal of the American College of Veterinary Radiology and the International Veterinary Radiology Association*, *46*(1), 44–48.

Reetz, J. A., Maï, W., Muravnick, K. B., Goldschmidt, M. H., & Schwarz, T. (2006). Computed tomographic evaluation of anatomic and pathologic variations in the feline nasal septum and paranasal sinuses. *Veterinary Radiology & Ultrasound: The Official Journal of the American College of Veterinary Radiology and the International Veterinary Radiology Association*, *47*(4), 321–327.

Roberts, N., Puddephat, M. J., & McNulty, V. (2000). The benefit of stereology for quantitative radiology. *British Journal of Radiology*, *73*(871), 679–697.

Sadeghinezhad, J., Zadsar, N., & Hasanzadeh, B. (2018). Morphometric changes in the spinal cord during prenatal life: a stereological study in sheep. *Anatomical Science International*, *93*(2), 269–276.

Sahin, B., & Ergur, H. (2006). Assessment of the optimum section thickness for the estimation of liver volume using magnetic resonance images: a stereological gold standard study. *European Journal of Radiology*, *57*(1), 96–101.

Saigal, R. P., & Khatra, G. S. (1977). Paranasal sinuses of the adult buffalo (*Bubalus bubalis*). *Anatomischer Anzeiger*, *141*(1), 6–18.

Saunders, J. H., Zonderland, J. L., Clercx, C., Gielen, I., Snaps, F. R., Sullivan, M., vanBree, H., & Dondelinger, R. F. (2002). Computed tomographic findings in 35 dogs with nasal aspergillosis. *Veterinary Radiology & Ultrasound: The Official Journal of the American College of Veterinary Radiology and the International Veterinary Radiology Association*, *43*(1), 5–9.

Seddek, A. M., Abedellaah, B., & Awaad, A. S. (2014). Computed tomography and dissection anatomy of the frontal and maxillary sinuses in native Egyptian goats. *Indian Journal of Veterinary Surgery*, *35*, 12–16.

Shojaei, B., Nazem, M. N., & Vosough, D. (2008). Anatomic reference for computed tomography of the paranasal sinuses and their openings in the rayini goat. *Iranian Journal of Veterinary Surgery*, *3*, 77–85.

Sisson, S., & Grossman, J. D. (1975). Ruminant osteology. In: R Getty (Ed.), *Sisson and Grossman's the anatomy of the domestic animals* (5th ed.). WB Saunders, pp 785–786.

Smallwood, J. E., Wood, B. C., Taylor, W. E., & Tate, L. P. Jr (2002). Anatomic reference for computed tomography of the head of the foal. *Veterinary Radiology & Ultrasound: The Official Journal of the American College of Veterinary Radiology and the International Veterinary Radiology Association*, *43*(2), 99–117.

Snyman, M. A. (2014). *South African sheep breeds: Ile de France sheep*. Infopack ref. 2014/018. Grootfontein Agricultural Development Institute.

Solano, M., & Brawer, R. (2004). CT of the equine head: Technical considerations, anatomical guide, and selected diseases. *Clinical Techniques in Equine Practice*, *3*, 374–388.

Tohidifar, M., Goodarzi, N., & Masoudifard, M. (2020). Anatomy of the head in the Saanen goat: a computed tomographic and cross-sectional approach. *Anatomical Science International*, *95*(3), 408–419.

Tucker, R., Windley, Z. E., Abernethy, A. D., Witte, T. H., Fiske-Jackson, A. R., Turner, S., Smith, L. J., & Perkins, J. D. (2016). Radiographic, computed tomographic and surgical anatomy of the equine sphenopalatine sinus in normal and diseased horses. *Equine Veterinary Journal*, *48*(5), 578–584.

Wang, X., Liu, A., Zhao, J., Elshaer, F. M., & Massoud, D. (2021). Anatomy of the skull of saanen goat. An anesthesiology and stereology approach. *International Journal of Morphology*, *39*, 423–429.

Zhu, L., Shi, X., Wang, J., & Chen, J. (2014). A morphometric study on the skull of donkey (*Equus asinus*). *International Journal of Morphology*, *32*, 1306–1310.

How to cite this article: Masoudifard, M., Zehtabvar, O., Modarres, S. H., Pariz, F., & Tohidifar, M. (2022). CT anatomy of the head in the Ile de France sheep. *Veterinary Medicine and Science*, *8*, 1694–1708. https://doi.org/10.1002/vms3.834